

High efficiency surface-conducted field emission from a ZnO nanotetrapod and MgO nanoparticle composite emitter

Ke Qu, Chi Li, Kai Hou, Xiayi Yang, Jin Zhang et al.

Citation: *Appl. Phys. Lett.* **93**, 253501 (2008); doi: 10.1063/1.3046785

View online: <http://dx.doi.org/10.1063/1.3046785>

View Table of Contents: <http://apl.aip.org/resource/1/APPLAB/v93/i25>

Published by the [American Institute of Physics](#).

Related Articles

Effective large-area free-standing graphene field emitters by electrophoretic deposition

Appl. Phys. Lett. **101**, 183107 (2012)

Quasi-monochromatic field-emission x-ray source

Rev. Sci. Instrum. **83**, 094704 (2012)

Analysis of field-emission from a diamond-metal-vacuum triple junction

J. Appl. Phys. **112**, 066102 (2012)

Screened field enhancement factor for a tall closely spaced array of identical conducting posts and implications for Fowler-Nordheim-type equations

J. Appl. Phys. **111**, 096102 (2012)

Homogeneity improvement of field emission beam from metallic nano-tip arrays by noble-gas conditioning

Appl. Phys. Lett. **99**, 073101 (2011)

Additional information on *Appl. Phys. Lett.*

Journal Homepage: <http://apl.aip.org/>

Journal Information: http://apl.aip.org/about/about_the_journal

Top downloads: http://apl.aip.org/features/most_downloaded

Information for Authors: <http://apl.aip.org/authors>

ADVERTISEMENT



Goodfellow
metals • ceramics • polymers • composites
70,000 products
450 different materials
small quantities fast

www.goodfellowusa.com

High efficiency surface-conducted field emission from a ZnO nanotetrapod and MgO nanoparticle composite emitter

Ke Qu,¹ Chi Li,¹ Kai Hou,¹ Xiayi Yang,¹ Jin Zhang,¹ Wei Lei,^{1,a)} Xiaobing Zhang,¹ Baoping Wang,¹ and X. W. Sun^{2,b)}

¹Display R&D Center, School of Electronic Science and Engineering, Southeast University, Nanjing 210096, People's Republic of China

²School of Electrical and Electronic Engineering, Nanyang Technological University, Nanyang Avenue, Singapore 639798, Singapore

(Received 18 September 2008; accepted 22 November 2008; published online 24 December 2008)

We report a surface-conducted field emitter made of a ZnO nanotetrapod and MgO nanoparticle composites with a high emission efficiency ($\sim 100\%$) and current (3.77 mA at a gate voltage of 100 V and anode voltage of 1800 V). The fabrications of the triode structure with a 10×10 pixel array and corresponding driving method have been proposed. The electron trajectories are simulated according to the structure. Individual pixel addressing can be achieved by a sequential scanning mode. Display of moving images employing this triode structure was demonstrated. The results are of significance to the development of ZnO based triode field emitters. © 2008 American Institute of Physics. [DOI: 10.1063/1.3046785]

Cold cathode field emission (FE) has attracted much attention for its application in a wide range of FE devices such as field emission display (FED), x-ray source, vacuum microwave amplifiers, etc. Over the years, various kinds of cold cathodes have been developed, for example, Spindt-type field emitter arrays,¹ metal-insulator-metal cathode,² and one-dimensional nanomaterial FE cathode.³

Recently, Geis *et al.*^{4,5} reported a FE with an ultralow electric field of 10 V/cm from a surface emission cathode. Nomura *et al.*⁶ reported a practical surface-conducted field emission (SCFE) cathode in 1996, based on which, Canon and Toshiba have showcased a 36 in. surface-conduction emission display panel in 2005.^{7,8} However, low emission efficiency is a serious drawback to realize practical and commercial SCFE panel. The emission efficiency of previously reported cathodes based on surface emission mechanism is in the range 0.1%–10%.^{7,9}

Very recently, we have reported a SCFE cathode made of ZnO nanotetrapod (ZNT) films with an emission efficiency of 60% (the efficiency in this paper refers to the percentage ratio of the anode current over the sum of the anode and gate current).¹⁰ Although the efficiency is much higher than those previously reported, there is still much room to improve to reach the ultimate efficiency of 100%. In this paper, we shall present an improved SCFE cathode made of ZNT and MgO nanoparticle composite with an efficiency close to 100%.

Figure 1 shows the schematic image of the screen-printed SCFE triode configuration and the pixel array. We use a 3 mm thick float law glass as the cathode substitute for making the triode structure. Before printing the Ag electrodes, the glass is cleaned in de-ionized water and ethanol. The cathode is composed of two vertical electrodes (25 μm thick, on the top called gate electrode, another called cathode electrode) separated by a 100 μm surface-conduction channel, with an area of 0.008 cm^2 (the width of the cathode electrode is 8 mm). The gates and cathodes are formed as

stripes by some Ag paste for vacuum fluorescent display (VFD) ($\sim 70\%$) from Guizhou Zhenhuaasia Pacific High Tech Electronic Materials Co., Ltd. The surface-conduction channel is made of ZNT and MgO nanoparticle composites. MgO nanoparticles ($\geq 98.5\%$, Analytical Reagent) used in this experiment were purchased commercially from Sinopharm Chemical Reagent Co., Ltd, and ZNTs were synthesized without any catalyst by vapor phase transport method in a horizontal tube furnace.¹¹ The ZnO–MgO (2:1 weight ratio) nanocomposite paste disperse in organic binders, which consisted of terpineol and ethyl cellulose using a homogenizer. The fabrication is described as follows. Cathode electrodes were screen-printed using Ag paste on a glass substrate, sintered at 560 $^\circ\text{C}$ for 4 h and cooled down to the room temperature. The dielectric layers were formed on the top of the cathode vertically. Subsequently, the gate electrodes were screen-printed on the dielectric layer as the same fabrication of cathode electrodes. In order to contact the two electrodes, ZnO–MgO paste was coated on the space between them. After baking at 500 $^\circ\text{C}$ for 30 min in a conventional oven in air and cooled down naturally, all organic vehicles were removed and a ZnO–MgO nanocomposite film was formed and also adhered well to the glass and Ag electrodes.

Figure 2(a) shows a low magnification scanning electron microscopy (SEM) top-view image of as-fabricated cathode, where we can identify the Ag and ZNT/MgO regions. Figure

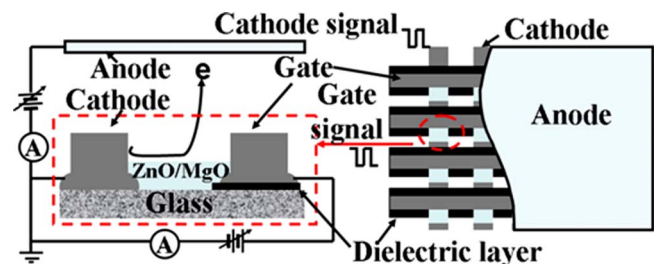


FIG. 1. (Color online) The schematic image of the SCFE triode configuration.

^{a)}Electronic mail: lw@seu.edu.cn.

^{b)}Electronic mail: exwsun@ntu.edu.sg.

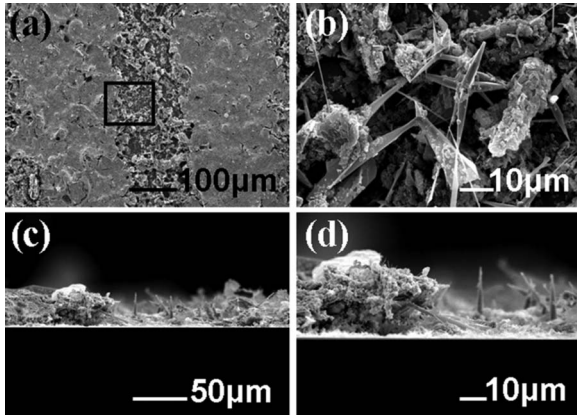


FIG. 2. (a) Low magnification SEM top-view picture of the ZNT/MgO film. (b) High magnification SEM top-view picture of the ZNT/MgO film in the rectangle of (a). (c) SEM cross-sectional picture of the ZNT/MgO film. (d) High magnification SEM of the triple junction.

2(b) shows a high magnification SEM image of a ZNT/MgO film in the rectangle of (a), where uniformly dispersed ZNTs and MgO nanopowders can be clearly seen. Figure 2(c) shows the cross section of the cathode, where the needle of the ZNT is perpendicular to the cathode plane. Figure 2(d) shows a high magnification SEM of Fig. 2(c).

FE testing was performed in a vacuum chamber at a pressure of $\sim 10^{-6}$ Pa. The space between the anode and the cathode was controlled by a 3 mm spacer. Electrical annealing (a few hundreds of volts) was applied on both the anode and gate electrode before real testing.¹² According to Fig. 1, a driving scheme for such a SCFE structure can be explained by a 10×10 pixel array. The device operates at a sequential scanning mode. The gate signal corresponds to scan signal (in row), and the cathode signal corresponds to the modulation signal (in column). For the nonaddressed row, the scan signal is zero, and all the rows of pixels are eliminated to the emitter. While for the address row, the scan signal is biased to the positive. In order to turn on the pixel, a negative bias is applied to the modulation signal. On the contrary, the modulation is biased to a positive to close the pixel.

The dependencies of the anode current and the gate current on gate voltage at different anode voltages are shown in Fig. 3(a). For a fixed anode voltage, both anode and gate current increase with the increase in gate voltage, much more quickly from 70 V and saturates at about 90 V. On the other hand, the anode current increases but the gate current decreases with the increase in anode voltage. Defining the ratio of the anode current and the total current (gate current plus anode current) as the emission efficiency, the calculated emission efficiency at different gate voltages and anode voltages is shown in Fig. 3(b). The emission efficiency is higher at a higher anode voltage, and the highest efficiency for different anode voltages occurs at a gate voltage in the range 72–77 V. The highest efficiency is close to 100% and the corresponding anode current is 1.2 mA, which are obtained at an anode voltage of 1800 V and gate voltage of 77 V. From the curve, we could see that the highest anode current is 3.77 mA at the anode voltage of 1800 V and gate voltage of 100 V and no emission current saturation was observed. The anode current per pixel inferred is $37.7 \mu\text{A}$, which is close to that of Canon and Toshiba's surface-conduction electron-emitter display (SED) ($40 \mu\text{A}$ anode current). But

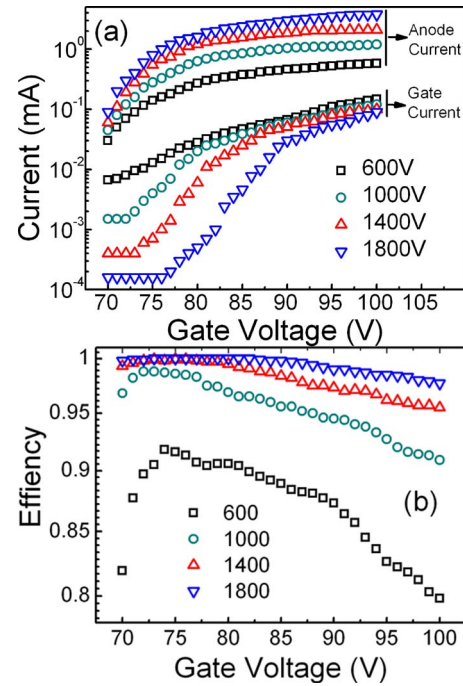


FIG. 3. (Color online) (a) The dependencies of the anode current and the gate current on gate voltage at different anode voltages. (b) Emission efficiency at different gate voltages and anode voltages.

our current density is larger than Canon and Toshiba's. The current density reported by Canon and Toshiba is about $3 \text{ mA}/\text{cm}^2$ at a very high gate field of $3666 \text{ V}/\mu\text{m}$, whereas a current density of $4.7 \text{ mA}/\text{cm}^2$ at a much lower gate field of $1 \text{ V}/\mu\text{m}$ was obtained for our SCFE. It is worth mentioning that the current density is also significantly improved compared to the report of Li and co-workers^{6–8,10} on SCFE using pure ZNTs ($0.6 \text{ mA}/\text{cm}^2$). Electron scattering is the main reason for SCFE, which can be explained as follows. Figure 4 is our electron trajectory simulation in a SCFE planar triode. The difference between the three pictures is the emitter material. In Fig. 4(a), there is no emitter between the cathode and the gate. As a result, when the gate voltage and the anode voltage are applied, only a little electron is emitted to the anode. When tetrapodlike ZnO is introduced as the emitter, a significant improvement of the electron sum is observed in Fig. 4(b). From the picture, we could see that the primary electrons emit from the cathode due to the strong

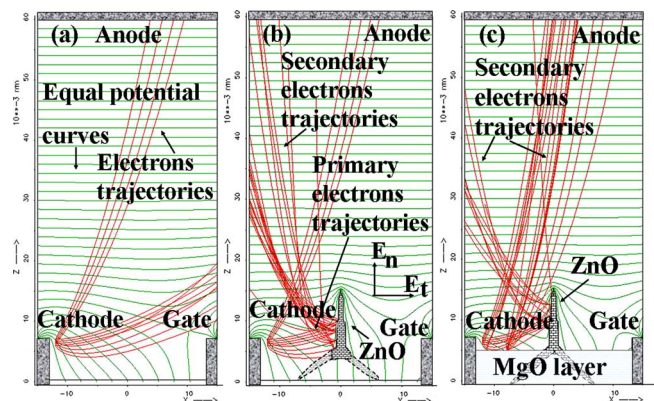


FIG. 4. (Color online) Simulations in the SCFE structure by different emitters. (a) None of the emitters. (b) Using a ZNT emitter. (c) Using a ZNT and a MgO nanoparticle composite emitter.

electric field between the cathode and the gate. When these primary electrons bombard on the ZNT, secondary electrons are generated. Because the tetrapodlike ZnO nanostructures have many protrusions, the longitudinal electric field (E_n) is formed around the ZNT, and part of the secondary electrons is collected by the anode. In order to increase the current efficiency, MgO is added into ZnO in Fig. 4(c). As randomness of the orientation of electron scattering, part of the loss electrons from the ZnO could bombard on the MgO layer and excite other secondary electrons from MgO. These secondary electrons could emit to the anode again because a very high yield of secondary electron emission (SEE) could be obtained as we used a MgO nanopowder film with a lot of voids (Fig. 2). Such a porous MgO film benefits generation of strong localized electric field, which further enhances the SEE.^{13,14} Meanwhile, adding MgO into ZnO makes the film more resistive, rendering a near zero gate current. It is worth mentioning that the emission can be turned off immediately when the applied gate voltage is removed, which is different from the cathode of Geis *et al.*^{4,5} This is because we have no electrodes under a glass substrate, i.e., no charge trapping in glass to maintain the voltage. In fact, the instant turn-off property is an advantage for the cathode being used in the FED panel with fast response time.

However, to realize an improvement of close to an order in current density (from 0.6 to 4.7 mA/cm²), there are other reasons that contribute to the enhancement of current density. One of the possible reasons may be triple junction, which plays a crucial role as the facilitator. In our configuration, a triple junction is formed between Ag, MgO/ZnO film, and vacuum,¹⁵ making a high field enhancement.^{16,17} However, an in-depth study will be discussed in our upcoming research.

Making use of this SCFE, a fully sealed 10×10 FED panel was fabricated. The test was carried out in a vacuum system with base pressure of 5×10⁻⁵ Pa. From both cathodes, addressing of individual pixel and display of characters and moving images were achieved. Figure 5 shows some Arabic numerals displayed on the panel. Each pixel could be accurately addressed and no interference is observed. The full emission image shown in Fig. 4 indicates that a good uniformity has been achieved.

In conclusion, we reported a surface emission cathode with high emission efficiency close to 100% and a large current about 3.7 mA with the gate voltage of 100 V. Low operation voltage was also obtained. 10×10 FED panel was fabricated to examine the practicability of the cathode. Testing experiment showed a uniform emission without crosstalk. This easy fabrication process provides a way to fabricate practical FED panel with high display quality.

The authors acknowledge the financial support from National Key Basic Research Program 973 (2003CB314702 and 2003CB314706), the Chinese 111 Project (B07027), and Program for New Century Excellent Talents in University



FIG. 5. (Color online) Arabic numerals displayed by the SCFE.

(NCET-04-0473 and NCET-05-0466). The sponsorship from Science and Engineering Research Council (Grant No. 0421010010) and from Agency for Science, Technology and Research, Singapore is gratefully acknowledged.

¹C. A. Spindt, *J. Appl. Phys.* **39**, 3504 (1968).

²D. Y. Lei and H. C. Ong, *Appl. Phys. Lett.* **91**, 211107 (2007).

³J. Zhou, N. S. Xu, S. Z. Deng, J. Chen, J. C. She, and Z. L. Zhong, *Adv. Mater. (Weinheim, Ger.)* **15**, 1539 (2003).

⁴M. W. Geis, N. N. Efremow, K. E. Krohn, J. C. Twichell, T. M. Lyszczarz, R. Kalish, J. A. Greer, and M. D. Tabat, *Nature (London)* **393**, 431 (1998).

⁵M. W. Geis, S. Deneault, K. E. Krohn, M. Marchant, T. M. Lyszczarz, and D. L. Cooke, *Appl. Phys. Lett.* **87**, 192115 (2005).

⁶T. Nomura, K. Sakai, E. Yamaguchi, M. Yamanobe, S. Ikeda, T. Hara, K. Hatanaka, and Y. Osada, *Proceedings of IDW '96*, 1996 (unpublished), p. 523.

⁷K. Yamamoto, I. Nomura, K. Yamazaki, S. Uzawa, and K. Hatanaka, *SID Int. Symp. Digest Tech. Papers* **36**, 1933 (2005).

⁸T. Oguchi, E. Yamaguchi, K. Sasaki, K. Suzuki, S. Uzawa, and K. Hatanaka, *SID Int. Symp. Digest Tech. Papers* **36**, 1929 (2005).

⁹K. Hou, C. Li, W. Lei, X. Zhang, W. Gu, and D. den Engelsen, *Nanotechnology* **18**, 335204 (2007).

¹⁰C. Li, K. Hou, W. Lei, X. Zhang, B. Wang, and X. W. Sun, *Appl. Phys. Lett.* **91**, 163502 (2007).

¹¹Z. Zhang, H. Yuan, Y. Gao, J. Wang, D. Liu, J. Shen, L. Liu, W. Zhou, S. Xie, X. Wang, X. Zhu, Y. Zhao, and L. Sun, *Appl. Phys. Lett.* **90**, 153116 (2007).

¹²L. Wei, X. Zhang, and Z. Zuoya, *J. Vac. Sci. Technol. B* **25**, 608 (2007).

¹³H. Jacobs, *Phys. Rev.* **84**, 877 (1951).

¹⁴J. M. Millet, *Phys. Rev. A* **52**, 433 (1995).

¹⁵M. Chhowalla, C. Ducati, N. L. Rupesinghe, K. B. K. Teo, and G. A. J. Amaratunga, *Appl. Phys. Lett.* **79**, 2079 (2001).

¹⁶D. S. Mao, X. Wang, W. Li, X. H. Liu, Q. Li, J. F. Xu, and K. Okano, *J. Vac. Sci. Technol. B* **18**, 2420 (2000).

¹⁷M. S. Chung, S. C. Hong, P. H. Cutler, N. M. Miskovsky, B. L. Weiss, and A. Mayer, *J. Vac. Sci. Technol. B* **24**, 909 (2006).